# Triazine-Based Type-II Photoinitiating System for Free Radical Photopolymerization: Mechanism, Efficiency, and Modeling

Julien Christmann, Xavier Allonas, Christian Ley, Ahmad Ibrahim, Céline Croutxe-Barghorn

DOI: 10.1002/macp.((insert number))

**Full Paper**

# Triazine-Based Type-II Photoinitiating System for Free Radical Photopolymerization: Mechanism, Efficiency and Modeling

*Dedicated to Yusuf Yagci at the occasion of his 65th anniversary*

Julien Christmann, Xavier Allonas*, Christian Ley, Ahmad Ibrahim, Céline Croutxé-Barghorn

J. Christmann, Pr. X. Allonas, Pr. C. Ley, Dr. A. Ibrahim, Pr. C. Croutxé-Barghorn
Laboratory of Macromolecular Photochemistry and Engineering
3b rue Alfred Werner, 68093 Mulhouse, France
E-mail: xavier.allonas@uha.fr

Isopropylthioxanthone, a versatile photoinitiator for free radical photopolymerization, is combined with a triazine derivative in a Type-II photoinitiating system (PIS). Initiation ability of this system for acrylate photopolymerization is assessed using a diacrylate monomer. Involvement of a photoinduced electron transfer mechanism is demonstrated by time-resolved spectroscopic measurements. Further insights in this mechanism are obtained through the use of a photopolymerization kinetic model taking into account the main reaction steps from the absorption of photons to the formation of the polymer. Prediction ability of the model is also tested with different initial concentrations of photoinitiator and co-initiator, as well as a different triazine derivative. This last experiment reveals the noticeable role of back electron transfer in the free radical photopolymerization mechanism of Type-II PIS.

FIGURE FOR ToC_ABSTRACT

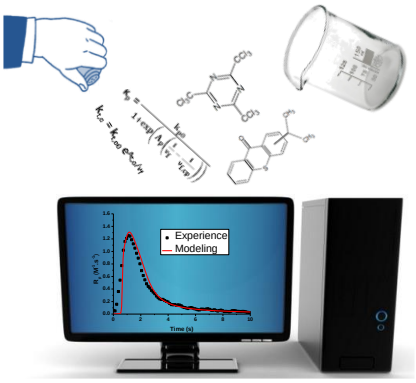

# 1. Introduction

Use of light for the synthesis of materials is an old topic: Egyptians used photocured bitumen of Judea to protect their mummies during the Antiquity.[1] Impressive progresses have been made since and photoinduced synthesis of materials is nowadays a large-scale industrial area. Among the large number of fields covered by this technology, radical photopolymerization has emerged as an attractive process for a wide range of applications such as coatings, varnishes, dental materials, graphic arts, laser direct imaging, holographic recording, etc.[1-6] Indeed, light irradiation provides numerous advantages over classic thermal operations: spatio-temporal control of the reaction, room temperature and solvent-free process, cost reduction… Light initiation of such a process is enabled by the use of a photoinitiating system (PIS). It converts photons into chemical energy through the production of radicals capable of reacting with acrylic monomers to initiate macromolecular chains. Three main families of PIS have been developed, each with their own advantages and limitations.[2,4-9] Type-I PIS rely on the photoinduced dissociation of the initiator to produce primary radicals. Despite a high quantum yield of radical production, typical bond dissociation energies require the use of UV lamps that are known to be harmful and to release ozone in the atmosphere. Therefore, Type-II photoinitiating systems (PIS) have been developed, which combine a photoinitiator (PI) able to absorb light and a co-initiator capable of reacting with the excited photoinitiator through hydrogen abstraction or electron transfer. Nevertheless, radical production is limited by the diffusion of the species into the viscous monomer medium and competition of the bimolecular reaction with PI deactivation pathways. In the case of hydrogen abstraction, hydrogenated PI radicals (PIH$^{\bullet}$, such as ketyl radicals) could also act as terminating agents and reduce final conversion.[10-11] Photocyclic initiating systems (PCIS) have then been developed in order to combine advantages of previous PIS, i.e. high radical production quantum yield under visible light. A redox additive is added to a Type-II photoinitiator/co-initiator system with the aim to react with the photoproducts created during the photochemical reaction. It has three main advantages: i) the fundamental state of the

PI is regenerated and can participate to a new cycle, ii) supplementary initiating radicals are produced, iii) potential terminating agents are consumed. Among the numerous PCIS redox additives reported into the literature, triazine derivatives (Tz) have been extensively used as electron-acceptors in combination with amines[12-17], thiols[18] or borate salts[18-21]. They have been found to enhance final conversion and rate of polymerization by reacting with the semi-reduced form of the PI. Indeed, fundamental state of the PI is regenerated and can participate to a new cycle while the semi-reduced form of the triazine ($Tz^{\bullet -}$) is expected to produce a triazinyl initiating radical ($Tz_{-Cl}^{\bullet}$) by dissociation of a C–Cl bond.[22] According to their electron acceptor nature, triazines would be able to react directly with an excited photoinitiator to generate triazinyl radicals. It has been reported that triazine A (TA) is not able to initiate acrylate photopolymerization when combined to several different dyes.[12-13] However, recent studies have proved that triazine derivatives are actually efficient to act as co-initiators, via a photoinduced electron transfer from the singlet state of pyrromethene derivatives.[15-17] Interestingly, isopropylthioxanthone (ITX) which is one of the most versatile photoinitiator for free radical photopolymerization (FRP)[23] has never been combined with triazine derivatives in a two-component photoinitiating system for FRP, although that such a combination has been studied for photoacid generation.[24]

In the present paper, we studied the ability of a Type-II photoinitiating system combining isopropylthioxanthone (ITX) as photoinitiator and 2,4,6-tris(chloromethyl)-1,3,5-triazine (triazine S, TS) as electron-accepting co-initiator to initiate acrylate photopolymerization. First, initiating ability of the system was studied with the LED-induced radical polymerization of a diacrylate monomer. Then, the nature of the photochemical interaction between ITX and TS was assessed by time-resolved spectroscopic measurements. In order to get more insights into the key-steps of the actual initiating mechanism with triazine derivatives, we adapted a FRP kinetic model in order to take into account specificities of such a Type-II PIS.

## 2. Experimental Section

### **2.1.** Materials

Isopropylthioxanthone (ITX) purchased from Fluka was a mixture of 2- and 4-isopropylthioxanthone (75 % and 25 %, respectively, as checked by $^{1}$H-NMR). 2,4,6-tris(chloromethyl)-1,3,5-triazine (TS) and 2-(4'-methoxyphenyl)-4,6-bis(trichloromethyl)-1,3,5-triazine (TA) were gift from PCAS (Longjumeau, France). Ethoxylated bisphenol A diacrylate (SR349) was supplied by Sartomer. Dimethylsulfoxide (DMSO, ≥ 99.8 %), butyronitrile (BuCN, ≥ 99.0 %), butyl acrylate (BA, ≥ 99.5 %) and 2,6-diphenyl-4-(2,4,6-triphenyl-1-pyridinio)phenolate,2,6-diphenyl-4-(2,4,6-triphenylpyridinio)phenolate (Reichardt's dye, 90 %) were purchased from Sigma-Aldrich. Acetonitrile (MeCN, ≥ 99.0 %) was supplied by Biosolve. All chemicals were used as received. Structures of the main compounds are given in Scheme 1.

### **2.2.** Experimental Methods

Formulations for kinetic analysis were based on a SR349 with eventually 10 wt% DMSO mixture. For Type-I PIS, 0.5 or 1 wt% (based on the resin total weight) of TPO was introduced. For Type-II PIS, different amounts of ITX and triazine (TS or TA) were introduced. Formulations were kept in the dark and stirred overnight.

Photopolymerization kinetics and monomer conversions were followed by real-time FTIR spectroscopy using a Vertex 70 from Bruker Optics operating in rapid scan mode and being equipped with a nitrogen liquid cooled MCT detector.[25-26] The sampling interval was 0.12 s and the resolution 4 $cm^{-1}$. In order to prevent the diffusion of atmospheric oxygen into the

sample during exposure, laminate experiments were carried out by placing the formulation between two polypropylene films and two $BaF_2$ pellets. Thickness of the sample was adjusted by using a 25 µm Teflon spacer. The irradiation was provided by a 395 nm LED device (Roithner LaserTechnik). The intensity of the LED was measured using a calibrated fiber optic spectrometer (Ocean Optics, USB4000) on which a PP film and a $BaF_2$ crystal were placed in order to measure the intensity actually reaching the sample. Kinetics of photopolymerization were measured by following the disappearance of the C=C bond stretching vibration band at 1637 $cm^{-1}$ and degree of conversion was calculated as:

$$\text{Conv}(\%) = \frac{(A_{1637})_0 - (A_{1637})_t}{(A_{1637})_0} \times 100 \quad (1)$$

where $(A_{1637})_0$ and $(A_{1637})_t$ are, respectively, the areas of the 1637 $cm^{-1}$ vibration band of the sample before exposure and at a given irradiation time $t$. Rate of polymerization $R_p$ (in M $s^{-1}$) was obtained from the Conv(%) vs time curve and the initial acrylate double bonds concentration in the formulation $[DB]_0$:

$$R_p = \frac{d\text{Conv}(\%)}{dt} \times \frac{[DB]_0}{100} \quad (2)$$

Conversion data were smoothed (adjacent-averaging method – 5 points) in order to avoid spikes in the $R_p$ curve due to local fluctuations of the conversion values, especially at early times. Each experiment was repeated at least three times in order to ensure a good reproducibility and presented results are the average of these data.

Dark polymerization experiments were performed with formulations containing 0.5 and 1 wt% TPO in pure SR349, by cutting the light irradiation at various time in the autoacceleration region (4, 4.5 and 5 s for 0.5 wt%; 2.25, 2.5 and 3 s for 1 wt%) while carrying on the RT-FTIR recording. Conv(%) and $R_p$ were obtained in the same way as for illuminated experiments.

Nanosecond transient absorption experiments were performed with an Edinburgh laser flash photolysis system. It combines a 50 W xenon lamp (Xe 900), a TM300 monochromator and a photomultiplier tube monitored by a digital oscilloscope. Light excitation was ensured by the third harmonic (355 nm) of a Continuum Surelite Nd:YAG pulsed laser operating at 10 Hz. Quenching and transient absorption spectra recorded in presence of ITX were obtained with an incident energy of 4 – 6 mJ and initial optical density of ITX of 0.12 at 355 nm. Self-quenching experiment was carried out at various concentrations of ITX. For direct excitation of TA (transient absorption spectrum and quenching by BA), initial optical density was set at 0.30 (at 355 nm) and incident energy at 18 – 20 mJ. All experiments were made in argon-saturated acetonitrile solutions. Quenching rate constants ($k_q$) were obtained by the usual Stern-Volmer treatment:

$$\tau^{-1} = \tau_0^{-1} + k_q[Q] \quad (3)$$

$\tau$ and $\tau_0$, respectively, refer to the triplet state lifetime with and without any quencher Q and [Q] is the concentration of this quencher in the cuvette.

UV-visible absorption spectra were recorded on a Cary 4000 spectrophotometer at room temperature in a quartz cuvette. ITX fluorescence lifetime was determined by time-correlated single photon counting, as detailed in [27]. Polymer volumetric mass $\rho_P$ was determined by picnometry and monomer glass transition temperature by differential scanning calorimetry (DSC), as explained in SI.

### **2.3.** Computational Methods

Photopolymerization kinetics were modeled with Wolfram Mathematica 9 software. Rate constants were defined as functions of the fractional free volume $v_f$ and differential equations

were numerically solved with the NDSolve function. Time evolution of all the species were generated in form of interpolating functions evaluated each 0.05 s. Conv(%) was directly calculated into the Mathematica notebook with Eq. 4 (where [DB] refers to the acrylate double bond concentration) and $R_p$ values were calculated after export with Eq. 2.

$$\text{Conv}(\%) = \frac{[\text{DB}]_0 - [\text{DB}]_t}{[\text{DB}]_0} \times 100 \quad (4)$$

## 3. Results and Discussion

### 3.1. Radical Photopolymerization Initiated by ITX / TS System

Triazine derivatives have often been considered in the development of photoinitiating systems for free radical photopolymerization of acrylates in Type-II PIS.[12-13,19] Therefore, it was found quite interesting to evaluate the initiating efficiency of triazine S (TS) using isopropylthioxanthone (ITX) as versatile photoinitiator.[23] Figure 1a displays the conversion of acrylate double bonds as a function of the irradiation time by a LED emitting at 395 nm with an incident irradiance of 10 mW $cm^{-2}$. The inhibition time is low and the maximum $R_p$ value is 0.82 M $s^{-1}$ at 1.9 s (Figure 1b). As can be seen, rapid and efficient conversion of acrylate double bonds was possible with a final conversion of 57 %, in agreement with the good reactivity already reported.[15,17]

### 3.2. Investigations of the Photochemical Initiating Mechanism

We have recently reviewed photochemical and electrochemical properties of ITX.[27] Due to the low lifetime of its singlet state (200 ps in MeCN), one can assume that photoinduced bimolecular interactions in the resin only occur from its triplet state ($\tau \approx 6$ µs in MeCN). The

interaction between triazine derivatives and ITX triplet state has been reported to occur through an energy transfer with a resulting triazine triplet state undergoing a homolytic dissociation of the C–Cl bond followed by a consecutive electron transfer between the radical moieties.[24] The triplet state energy $E_T$ of TS is 3.2 eV,[12] a value much higher than that of ITX ($E_T$ = 2.71 eV[24]). Therefore, the triplet-triplet energy transfer from ITX to TS appears thermodynamically disfavored, the Gibbs free energy variation of energy transfer being $\Delta G_{PEneT}$ = 0.49 eV. As TS presents a reduction potential similar to that of typical iodonium salts (-1.0 V / SCE measured in this work *vs.* -0.7 to -0.85 V / SCE for iodonium salts[17,27]), a similar electron transfer mechanism is expected to occur. The Gibbs free energy variation of such a reaction is given by the Rehm-Weller equation:[28-29]

$$\Delta G_{PEleT} = E_{ox}(ITX) - E_{red}(TS) - E_T + C \quad (5)$$

where $E_{ox}$(ITX) is the oxidation potential of ITX, $E_{red}$(TS) the reduction potential of TS. The coulombic term $C$ is generally neglected in polar solvents such as acetonitrile. Taking into account the properties of ITX ($E_{ox}$(ITX) = 1.51 V / SCE[27]), this leads to a $\Delta G_{PEleT}$ value of -0.20 eV. Thus, photoinduced electron transfer appears to be much more exergonic than energy transfer.

Quenching of $^3$ITX by TS was found to be quite effective, with a quenching rate constant $k_q$ of $3.1 \times 10^9$ $M^{-1}$ $s^{-1}$ in good agreement with the negative $\Delta G_{PEleT}$ previously calculated. In order to ensure this mechanism, transient absorption spectrum of ITX was monitored in presence of TS in acetonitrile (Figure 2). According to the transient spectrum of ITX previously reported in MeCN under similar conditions, absorption signals at 310 and 640 nm are attributed to the triplet-triplet absorption of ITX while the negative one at 380 nm corresponds to the photobleaching of the corresponding fundamental state.[27] The first clue indicating that the energy transfer is not the predominant process is given by the fact that the photobleaching at 380 nm doesn't totally recover in the time scale of the experiment (Figure 2). The long-lived

transient observed could be explained by the uncomplete recovery of $^{0}$ITX due to the formation of the ITX radical cation ($ITX^{\bullet+}$) through electron transfer. This contention is confirmed by the apparition of a new band at 340 nm consecutively to the ITX triplet decay which has been previously assigned to $ITX^{\bullet+}$.[27] An additional transient appears within the same time scale at 290 nm which is similar to that reported for a triazinyl radical ($Tz_{\text{-Cl}}^{\bullet}$)[22] and checked by ourselves by direct irradiation of TA at 355 nm (Figure S1, see SI). This new band can then be confidently attributed to the triazinyl radical of TS ($TS_{\text{-Cl}}^{\bullet}$). Analysis of $^{3}$ITX decay and signal growth at 290 and 340 nm is also interesting and reveals similar kinetics (Figure S2), indicating that $TS_{\text{-Cl}}^{\bullet}$ and $ITX^{\bullet+}$ are produced directly from the quenching reaction of $^{3}$ITX. As photoinduced electron transfer from $^{3}$ITX to TS would produce $ITX^{\bullet+}$ and $TS^{\bullet-}$, this analysis shows that the latter loses a chloride anion to form the triazinyl. Two explanations can be proposed: i) the dechlorination of $TS^{\bullet-}$ is faster than reported rate constant values ($k_{\text{-Cl}}$ = 8 – 20 × $10^{4}$ $s^{-1}$[22]) and we are not able to detect the short-living $TS^{\bullet-}$ with our setup; ii) the band at 290 nm is a mix of the signals of $TS^{\bullet-}$ and $TS_{\text{-Cl}}^{\bullet}$ (probably presenting similar spectral properties as their structures are alike).

In order to characterize the initiation mechanism of an acrylate photopolymerization reaction by triazinyl radicals, the reaction rate constant between triazinyl radicals and an acrylate (*i.e.* the initiation rate constant $k_i$) was measured by LFP. The triazinyl radical was obtained by direct UV excitation of TA in the presence of increasing amounts of butyl acrylate BA (Figure 3). A value of almost 3 × $10^{4}$ $M^{-1}$ $s^{-1}$ was found, showing that triazinyl radicals $TA_{\text{-Cl}}^{\bullet}$ are efficient to initiate FRP of acrylates. As $TA_{\text{-Cl}}^{\bullet}$ looks more stabilized than $TS_{\text{-Cl}}^{\bullet}$ thanks to an extended conjugated system, this value is considered as a lower limit of $k_i$ for $TS_{\text{-Cl}}^{\bullet}$.

This photochemical study demonstrated that the interaction between $^{3}$ITX and TS is governed by a photoinduced electron transfer mechanism and that the triazinyl radicals generated from

the fast dechlorination of $TS^{\bullet-}$ are efficient to initiate the photopolymerization of an acrylate monomer (Scheme 2).

### 3.3. Kinetic Modeling of FRP Initiated by a Triazine-Based Type-II PIS

As seen before, triazine derivatives behave as efficient co-initiators for Type-II photoinitiating systems. It is quite interesting to model the free radical photopolymerization by taking into account not only the photochemical mechanism of reaction but also the effect of this mechanism on the photopolymerization kinetics. Indeed, different processes are known to affect the conversion-time evolution during FRP reaction such as auto-acceleration and –deceleration[30-32] as well as termination by reaction diffusion. [30,33-45] Taking into account these effects into a kinetic model requires to consider the change in the rate constants during the photopolymerization within a free radical photopolymerization model as described in the literature[46-51] and recently used to predict kinetic rate constants during dark polymerizations experiments under oxygen diffusion[52] and model layer-by-layer UV-curing.[53] Complete description of the model can be found in SI. One of its main advantages is that it does not stick on the pseudo-steady-state approximation which was found to be invalid from the onset of the autoacceleration region.[46] However, a relatively high number of parameters is required to run properly such simulation. Among them, some are easily accessible by experiment (glass transition temperature $T_g$, density $\rho$, resin viscosity $\eta$, etc.) and some others can be found in the literature (initiation kinetic constant without diffusional control $k_{i0}$, thermal expansion coefficient $\alpha$, etc.). Kinetic parameters governing the evolution of the rate constants (especially reaction diffusion termination parameter $R_{rd}$, exponential coefficients $A$ and critical free volumes $\nu_{f,c}$) are more specific to this work. Experimental procedures have then been proposed to determine some of them using a Type-I PIS, while the others can be reasonably approximated.[48-50,54] It was decided to determine these parameters with the Type-I photoinitiator diphenyl 2,4,6-trimethylbenzoyl phosphine oxide (TPO). Complete explanations

of the parameter determination as well as the description of the Type-I PIS kinetic model for TPO (mechanism, differential equations, fit to experimental data…) are given in SI. It should be pointed out that 10 wt% of DMSO was introduced into the acrylate resin in order to avoid premature vitrification that would limit the analysis of the photochemical impact on the polymerization. Knowing this set of polymerization parameters, it is then possible to replace photodissociation of a Type-I PIS by reactions specific to Type-II PIS in the kinetic model.

From the photochemical study, it could be assumed that initiating triazinyl radicals and ITX radical anions are produced through a photoinduced electron transfer from ITX to TS. Then, the mechanism, proposed in Scheme 2, was transcribed into a set of differential equations describing the change of the concentration in $^{0}$ITX, $^{1}$ITX, $^{3}$ITX, TS, $TS^{\bullet-}$, $TS_{\text{-Cl}}^{\bullet}$ and $ITX^{\bullet+}$ (see SI). All other polymerization parameters (except $k_{i0}$ taken from our photochemical study) were the same as discussed above. It should be noted that by contrast to TPO, only one initiating radical ($TS_{\text{-Cl}}^{\bullet}$) is produced during the photochemical reaction.

Specific photochemical parameters of ITX are required to solve the whole differential system. From solvatochromic study using Reichardt's dye, the polarity parameter $E_T(30)$ of the mixture of SR349 with 10 wt% of DMSO was found to be 42.9 kcal mol$^{-1}$ , quite close to that of butyronitrile (42.5 kcal mol$^{-1}$ [55]).[56] Thus, the medium-dependent parameters such as $\varepsilon$, singlet and triplet lifetimes, self-quenching rate constant $k_{sq}$ ($4.5 \times 10^{8}$ M$^{-1}$ s$^{-1}$ )… were determined in that butyronitrile. Triplet-triplet annihilation was also taken into account, as its rate constant is quite high ($k_{TTA} = 7 \pm 3 \times 10^{9}$ M$^{-1}$ s$^{-1}$ [57]). Expressions of the rate constants of singlet ($k_{dea1}$) and triplet ($k_{dea3}$) deactivation (by either radiative or non-radiative pathways) as well as intersystem crossing rate constant ($k_{ISC}$) have been determined in a previous study (Eqs. 6 - 8).[58]

$$k_{ISC} = \Phi_T / \tau_S \quad (6)$$

$$k_{dea1} = 1 / \tau_S - k_{ISC} \quad (7)$$

$$k_{dea3} = 1 / \tau_T \quad (8)$$

$\Phi_T$ refers to the triplet state formation quantum yield of ITX and $\tau_s$ and $\tau_T$ its singlet and triplet state lifetime respectively. The $TS^{\bullet -}$ dissociation rate constant has been reported equal to $1.0 \times 10^5$ $s^{-1}$.[22] As it was proved that $ITX^{\bullet +}$ can be quenched by hydrogen-donor species,[27] we also assume a similar reaction with impurities and stabilizers inherently present in the formulation. This reaction produces radicals reactive towards oxygen and other radical species, and the protonated form of $ITX^{\bullet +}$, finally able to go back to $^0$ITX after deprotonation (see the associated reactions in SI).

At first was considered the electron transfer between $^3$ITX and TS as a diffusion-limited mechanism by setting $k_q$ equal to the initial $k_d$ value of the formulation ($3.2 \times 10^7$ $M^{-1}$ $s^{-1}$). The best fits are compared to experimental data in Figures 4.

From a general point of view, the model reproduces satisfactorily the shape of the conversion-time curve and the final conversion value (1 % of error). However, the obtained $R_p^{max}$ value is not yet sufficiently accurate to be satisfying (14 % of error). Indeed, the calculated rate of polymerization is higher than the experimental one, indicating that the amount of radicals actually available is lower than calculated. Therefore, one should take into account a possible back electron transfer (bet) which could take place after the photoinduced electron transfer between triplet ITX and TS. bet could explain an experimental quantum yield of radical production ($\Phi_{rad}$) lower than that predicted by our model, even if other side reactions cannot be totally ruled out. Scheme 3 describes such mechanism. In the distinctive case of a dissociative radical anion such as triazine ones, dissociation of the semi-reduced species can take place before separation of the radical ion pair and prevent back-electron transfer (see complete mechanism in SI). $k_{-d}$ and $k_{sep}$ were taken equal to $0.8k_d$, according to the value proposed by

Rehm and Weller in their pioneering work.[29] As measured $k_q$ value for ITX + TS reaction was closed to $k_d$ in MeCN, we extracted the pure electron transfer rate constant ($k_{et}$) with Eq. 9.[59]

$$k_q = \frac{k_{et} \times k_d}{k_{et} + k_{-d}} \quad (9)$$

A value of -2.51 eV was found for the bet Gibbs free energy variation $\Delta G_{bet}$ by taking $E_{red}(ITX^{\bullet+}) \approx E_{ox}(ITX)$ and $E_{ox}(TS^{\bullet-}) \approx E_{red}(TS)$. As the maximum of the typical $\log(k_{PEleT}) = f(\Delta G_{PEleT})$ curve in Marcus' theory is located at $\Delta G_{PEleT} = -\lambda$ (with $\lambda$ the reorganization barrier, typically comprised between 1 and 2 eV[60]), it clearly indicates that this reaction relies to the inverted region of Marcus' theory, characterized by a decreasing $k_{et}$ value with decreasing $\Delta G_{PEleT}$.[60-63] The $k_{bet}$ value was adjusted by trial-and-error fit to the experimental data. A $k_{bet}$ value of $4.0 \times 10^6$ $s^{-1}$ was found for our system. As this value is lower than $k_d$ at early times, we decided to modify the expression of the rate constant of electron transfer between separated $ITX^{\bullet+}$ and $TS^{\bullet-}$ ($k_{radbet}$), initially taken equal to $k_d$. In order to take into account the diffusion control at longer times, we defined $k_{radbet}$ as:

$$k_{radbet} = \frac{k_{bet} \times k_d}{k_{bet} + k_{-d}} \quad (10)$$

According to this change, the $R_p^{max}$ value obtained is slightly increased (of about 0.017 M $s^{-1}$) but one can adjust $k_{bet}$ to $4.5 \times 10^6$ $s^{-1}$ in order to recover the agreement for both Conv(%) and $R_p$ curves (respectively 1 and 5 % of error), as displayed on Figures 5. As can be seen, introduction of the bet into our modeling has a noticeable effect on the $R_p$ curve and its absence may explain the higher $R_p^{max}$ initially calculated than the experimental one.

In order to get more insight into the effect of bet on the FRP process, the results for TS were compared to that obtained with TA. Because TA highly absorbs around 355 nm, it was not possible to analyze its photosensitized mechanism with ITX by LFP. However, positive $\Delta G_{PEneT}$ value of 0.19 eV ($E_T$ = 2.9 eV[12]) compared to $\Delta G_{PEleT}$ of -0.08 eV ($E_{red}$ = -1.12 V / SCE[16])

tends to indicate that a photoinduced electron transfer is also operating for ITX / TA system. The Type-II PIS model was used with parameters specific to TA (initial concentrations, $k_{et}$ extracted with Eq. 9 from the $k_q = 3.7 \times 10^9$ $M^{-1}$ $s^{-1}$ reported value[64]) and a $k_{bet}$ value of $7.5 \times 10^5$ $s^{-1}$ was found (Figure 6) for a $\Delta G_{bet}$ value of -2.63 eV. The $\Delta G_{bet}$ of TA being more negative than that of TS (corresponding to a more exergonic reaction), the $k_{bet}$ value is accordingly lower for TA than TS by virtue of the inverted region behavior.[60-63] Good agreement is also found for final conversion (1 % of error) and $R_p^{max}$ (2 % of error) values.

In order to assess the robustness of the kinetic model, it was decided to compare modeling results to experimental data while varying the initial concentration of ITX or TS. Tested systems are listed into Table 1 and results displayed in Figure 7. As can be seen, the modification of $[TS]_0$ is well reproduced by our model both for conversion (1 to 4 % of error on final conversion) and $R_p$ (4 to 10 % of error on $R_p^{max}$) curves. For ITX initial concentration, final conversion and $R_p^{max}$ are slightly over-estimated by the model. This can be explained by the uncertain nature of some photoproducts. Moreover, oxygen inhibition is not perfectly reproduced, especially at low ITX initial concentration. This could originate from side reactions involving peroxy radicals ROO$^\bullet$ produced during the reaction of radical species with oxygen (see the mechanism in the SI) which are not taken into account in the model as they are not totally understood yet.[65] However, trends are well reproduced in all cases and this model could be used for qualitative prediction of modifying PIS initial composition.

## 4. Conclusions

It was shown that triazine S can be combined with the ITX photoinitiator to initiate FRP of a diacrylate monomer. The photoinduced mechanism of initiation relies on an electron transfer from triplet ITX to TS, followed by TS radical anion dissociation to give initiating triazinyl radicals. Further insights into this complex mechanism were obtained by modeling the whole

FRP process initiated by this system, therefore adapting a kinetic model to initiation by Type-II PIS. It revealed that back electron transfer has a noticeable effect on the rate of polymerization. Comparison to results for a different triazine derivative also shows that the bet process relies to the well-known Marcus inverted region, as the electron transfer rate constant decreases with decreasing Gibbs free energy variation. Finally, modeling of different initial contents of ITX and TS reveals that the model could be used to qualitatively describe the effect over a range of concentrations. Transposing a model initially dedicated to initiation by Type-I PIS to that of a Type-II system offers new perspectives in the mechanistic study of complex photoinitiating systems such as photocyclic ones.

## Supporting Information

Supporting Information is available from the Wiley Online Library or from the author.

Acknowledgements: ANR and Mäder are fully acknowledged for financial support of the DeepCure project #ANR-13-CHIN-0004-01.

Received: Month XX, XXXX; Revised: Month XX, XXXX; Published online:
((For PPP, use "Accepted: Month XX, XXXX" instead of "Published online")); DOI: 10.1002/marc.((insert number)) ((or ppap., mabi., macp., mame., mren., mats.))

Keywords: photopolymerization, radical polymerization, kinetic modeling, initiation mechanism, photochemistry

References:


[1] C. Decker, *J. Coat. Technol.* **1987**, *59*, 97.

[2] J-P. Fouassier, *Photoinitiation, Photopolymerization, and Photocuring – Fundamentals and Applications*, Hanser/Gardner Publications, Munich, Germany **1995**.

[3] C. Decker, *Pigm. Resin Technol.* **2001**, *30*, 278.

[4] W. Schnabel, *Polymers and Light – Fundamentals and Technical Applications*, Wiley-VCH, Weinheim, Germany **2007**.

[5] X. Allonas, C. Croutxé-Barghorn, J-P. Fouassier, J. Lalevée, J-P. Malval, F. Morlet-Savary, in *Lasers in Chemistry*, Vol. 2 (Ed: M. Lackner), Wiley-VCH, Weinheim, Germany **2008**, Chap. 35.

[6] Y. Yagci, S. Jockusch, N. J. Turro, *Macromolecules* **2010**, *43*, 6245.

[7] J-P. Fouassier, X. Allonas, J. Lalevée, C. Dietlin, in *Photochemistry and Photophysics of Polymer Materials*, (Ed: N. S. Allen), Wiley, Hoboken, NJ, USA **2010**, chap. 10.

[8] J-P. Fouassier, J. Lalevée, *Photoinitiators for Polymer Synthesis*, Wiley-VCH, Weinheim, Germany **2012**.

[9] A. Ibrahim, L. H. Di Stefano, O. Tarzi, H. Tar, C. Ley, X. Allonas, *Photochem. Photobiol.* **2013**, *89*, 1283.

[10] H. Block, A. Ledwith, A. R. Taylor, *Polymer* **1971**, *12*, 271.

[11] D. G. Anderson, R. S. Davidson, J. J. Elvery, *Polymer* **1996**, *37*, 2477.

[12] C. Grotzinger, D. Burget, P. Jacques, J-P. Fouassier, *Macromol. Chem. Phys.* **2001**, *202*, 3513.

[13] C. Grotzinger, D. Burget, P. Jacques, J-P. Fouassier, *Polymer* **2003**, *44*, 3671.

[14] J-P. Fouassier, X. Allonas, D. Burget, *Prog. Org. Coat.* **2003**, *47*, 16.

[15] A. Ibrahim, C. Ley, O. I. Tarzi, J-P. Fouassier, X. Allonas, *J. Photopolym. Sci. Tec* **2010**, *23*, 101.

[16] O. I. Tarzi, X. Allonas, C. Ley, J-P. Fouassier, *J. Polym. Sci. Pol. Chem* **2010**, *48*, 2594.

[17] A. Ibrahim, C. Ley, X. Allonas, O. I. Tarzi, A. Chan Yong, C. Carré, R. Chevallier, *Photochem. Photobiol. Sci.* **2012**, *11*, 1682.

[18] J. Kabatc, K. Jurek, *Polymer* **2012**, *53*, 1973.

[19] J. Kabatc, M Zasada, J. Paczkowski, *J. Polym. Sci. Pol. Chem.* **2007**, *45*, 3626.

[20] J. Kabatc, Z. Czech, A. Kowalczyk, *J. Photoch. Phobio. A* **2011**, *219*, 16.

[21] J. Kabatc, K. Kostrzewska, K. Jurek, *Colloid. Polym. Sci.* **2015**, *293*, 1865.

[22] G. Pohlers, J. C. Scaiano, *Chem. Mater.* **1997**, *9*, 1353.

[23] S. Dadashi-Silab, C. Aydogan, Y. Yagci, *Pol. Chem.* **2015**, *6*, 695.

[24] G. Pohlers, J. C. Scaiano, E. Step, R. Sinta, *J. Am. Chem. Soc.* **1999**, *121*, 6167.

[25] C. Decker, K. Moussa, *Macromolecules* **1989**, *22*, 4455.

[26] A. Ibrahim, V. Maurin, C. Ley, X. Allonas, C. Croutxé-Barghorn, F. Jasinski, *Eur. Polym. J.* **2012**, *48*, 1475.

[27] J. Christmann, S. Shi, A. Ibrahim, C. Ley, C. Croutxé-Barghorn, M. Bessières, X. Allonas, *J. Phys.Chem. B*, DOI: 10.1021/acs.jpcb.6b11829.

[28] D. Rehm, A. Weller, *Ber. Bunsenges.Phys. Chem.* **1969**, *73*, 834.

[29] D. Rehm. A. Weller, *Isr. J. Chem.* **1970**, *8*, 259.

[30] E. Andrzejewska, *Prog. Polym. Sci.* **2001**, *26*, 605.

[31] G. Odian, *Principles of Polymerization*, 4th ed., Wiley-Interscience, Hoboken, NJ, USA **2004**.

[32] Y. Gnanou, M. Fontanille, *Organic and Physical Chemistry of Polymers*, Wiley-Interscience, Hoboken, NJ, USA **2008**.

[33] G. V. Schulz, *Z. Phys. Chem. (Munich)* **1956**, *8*, 290.

[34] M. Stickler, *Makromol. Chem.* **1983**, *184*, 2563.

[35] M. J. Ballard, D. H. Napper, R. G. Gilbert, D. F. Sangster, *J. Polym. Sci. Pol. Chem.* **1986**, *24*, 1027.

[36] M. Buback, B. Degener, B. Huckestein, *Makromol. Chem. Rapid. Commun.* **1989**, *10*, 311.

[37] M. Buback, *Makomol. Chem.* **1990**, *191*, 1575.

[38] W. D. Cook, *J. Polym. Sci. Pol. Chem.* **1993**, *31*, 1053.

[39] K. S. Anseth, C. M. Wang, C. N. Bowman, *Polymer* **1994**, *35*, 3243.

[40] K. S. Anseth, C. N. Bowman, N. A. Peppas, *J. Polym. Sci. Pol. Chem.* **1994**, *32*, 139.

[41] K. S. Anseth, C. M. Wang, C. N. Bowman, *Macromolecules* **1994**, *27*, 650.

[42] M. Buback, B. Huckestein, G. T. Russell, *Macromol. Chem. Phys.* **1994**, *195*, 539.

[43] K. S. Anseth, L. M. Kline, T. A. Walker, K. J. Anderson, C. N. Bowman, *Macromolecules* **1995**, *28*, 2491.

[44] M. Buback, *Macromol. Symp.* **1996**, *111*, 229.

[45] J. S. Young, C. N. Bowman, *Macromolecules* **1999**, *32*, 6073.

[46] C. N. Bowman, N. A. Peppas, *Macromolecules* **1991**, *24*, 1914.

[47] K. S. Anseth, C. N. Bowman, *Polym. React. Eng.* **1992-1993**, *1*, 499.

[48] M. D. Goodner, H. R. Lee, C. N. Bowman, *Ind. Eng. Chem.* **1997**, *36*, 1247.

[49] M. D. Goodner, C. N. Bowman, in *Solvent Free Polymerizations and Processes*, Vol. 713 (Eds: T. E. Long, M. O. Hunt), ACS Symposium Series, American Chemical Society, Washington, DC, USA **1999**, Chap. 14.

[50] M. D. Goodner, C. N. Bowman, *Macromolecules* **1999**, *32*, 6552.

[51] M. D. Goodner, C. N. Bowman, *Chem. Eng. Sci.* **2002**, *57*, 887.

[52] K. Taki, Y. Watanabe, H. Ito, M. Ohshima, *Macromolecule* **2014**, *47*, 1906.

[53] K. Taki, Y. Watanabe, T. Tanabe, H. Ito, M. Ohshima, *Chem. Eng. Sci.* **2017**, *158*, 569.

[54] J. Wong, K. Kaastrup, A. Aiguirre-Soto, H. D. Sikes, *Polymer* **2015**, *69*, 169.

[55] Y. Marcus, *The Properties of Solvents*, Wiley, Chichester, England **1998**.

[56] C. Reichardt, *Chem. Rev.* **1994**, *94*, 2319.

[57] G. Amirzadeh, W. Schnabel, *Makromol. Chem.* **1981**, *182*, 2821

[58] C. Ley, J. Christmann, A. Ibrahim, L. H. Di Stefano, X. Allonas, *Beilstein J. Org. Chem.* **2014**, *10*, 936.

[59] C. Ley, A. Ibrahim, X. Allonas, *Photochem. Photobio. Sci.* **2016**, *15*, 1054.

[60] N. J. Turro, V. Ramamurthy, J. C. Scaiano, *Principles of Molecular Photochemistry – An Introduction*, University Science Books, Sausalito, California, USA **2009**.

[61] R. A. Marcus, *J. Chem. Phys.* **1956**, *24*, 966.

[62] R. A. Marcus, *Annu. Rev. Phys. Chem.* **1964**, *15*, 155.

[63] R. A. Marcus, N. Sutin, *Biochim. Biophys. Acta* **1985**, *811*, 265.

[64] V. Charlot, A. Ibrahim, X. Allonas, C. Croutxé-Barghorn, C. Delaite, *Polym. Chem.* **2014**, *5*, 6236.

[65] R. Pynaert, J. Buguet, C. Croutxé-Barghorn, P. Moireau, X. Allonas, *Polym. Chem.* **2013**, *4*, 2475.

Schemes:

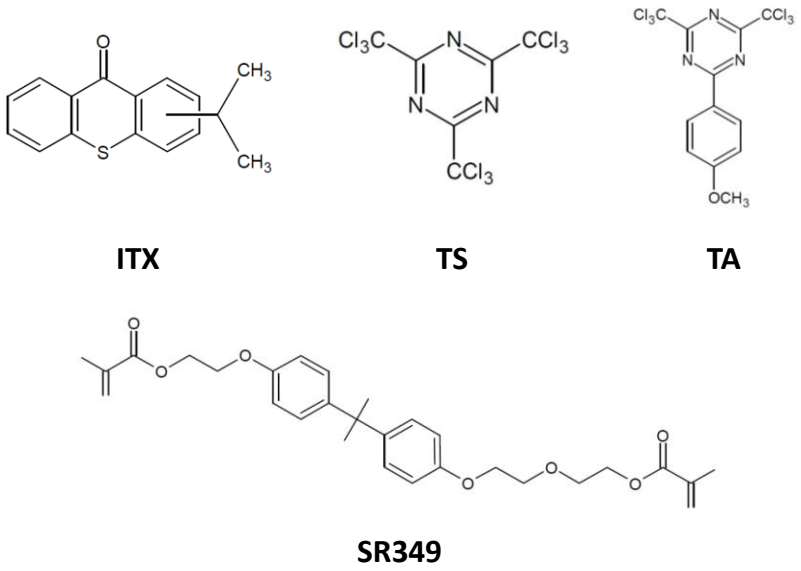


*Scheme 1*. Molecular structures of the main compounds used in this study.

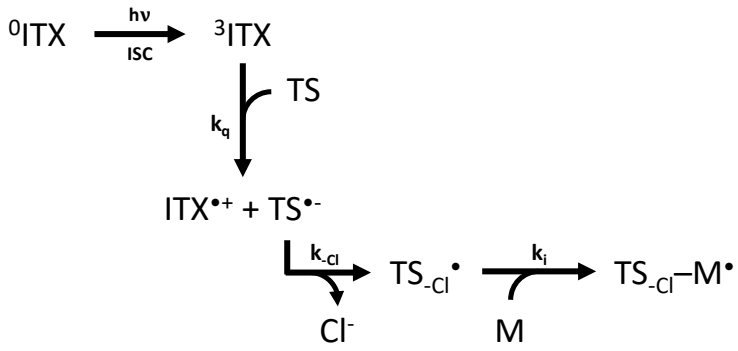


*Scheme 2*. Photoinitiation mechanism of the free radical polymerization reaction by ITX / triazine S (TS) initiating system.

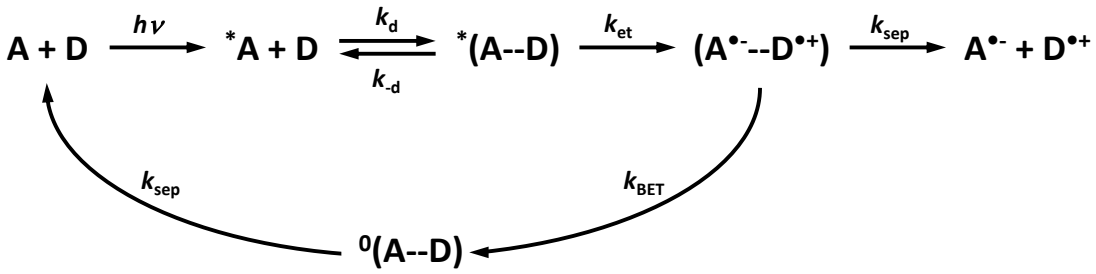


*Scheme 3*. Mechanism of photoinduced electron transfer with encounter complex, radical ion pair formation and back electron transfer.

Tables:

*Table 1.* Composition of the different ITX + TS systems tested (in SR349 + 10 wt% DMSO) and experimental polymerization results. Errors on modeling data with respect to experimental data are given in parenthesis.

| **System** | **ITX (wt%)** | **$[TS]_0$ (M)** | **Final Conv(%)** | **$R_p^{max}$ (M $s^{-1}$)** |
|---|---|---|---|---|
| 1 | 0.1 | $8 \times 10^{-3}$ | 74 % (3 %) | 1.03 (4 %) |
| 2 | 0.1 | $2 \times 10^{-2}$ | 77 % (1 %) | 1.33 (8 %) |
| 3 | 0.2 | $1.5 \times 10^{-2}$ | 80 % (4 %) | 1.64 (10 %) |

Figures:

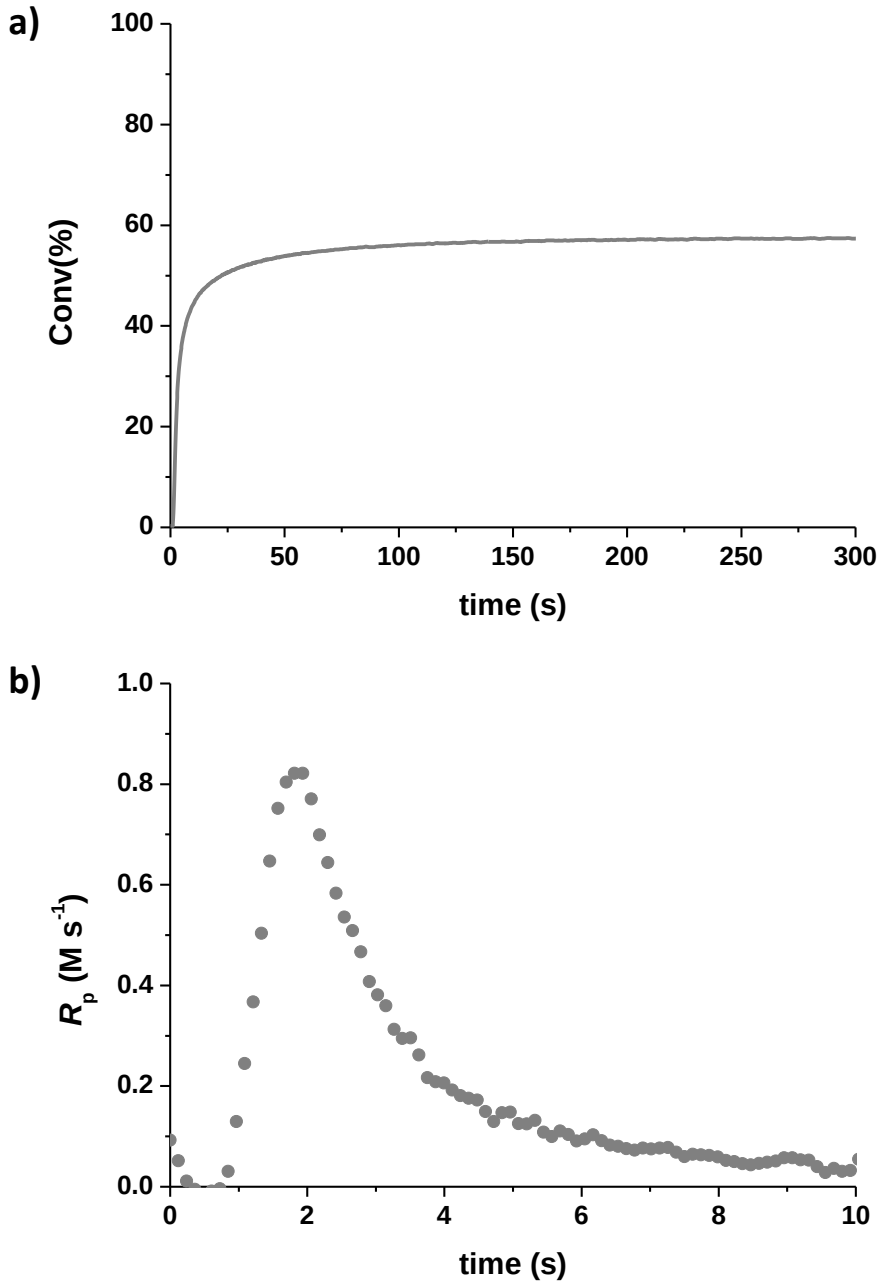


*Figure 1.* a) Acrylate double bond conversion curve and b) corresponding rate of polymerization upon LED exposure at 395 nm (irradiance = 10 mW cm$^{-2}$) – ITX / TS (0.1 wt% / 1.5 × 10$^{-2}$ M) in SR349.

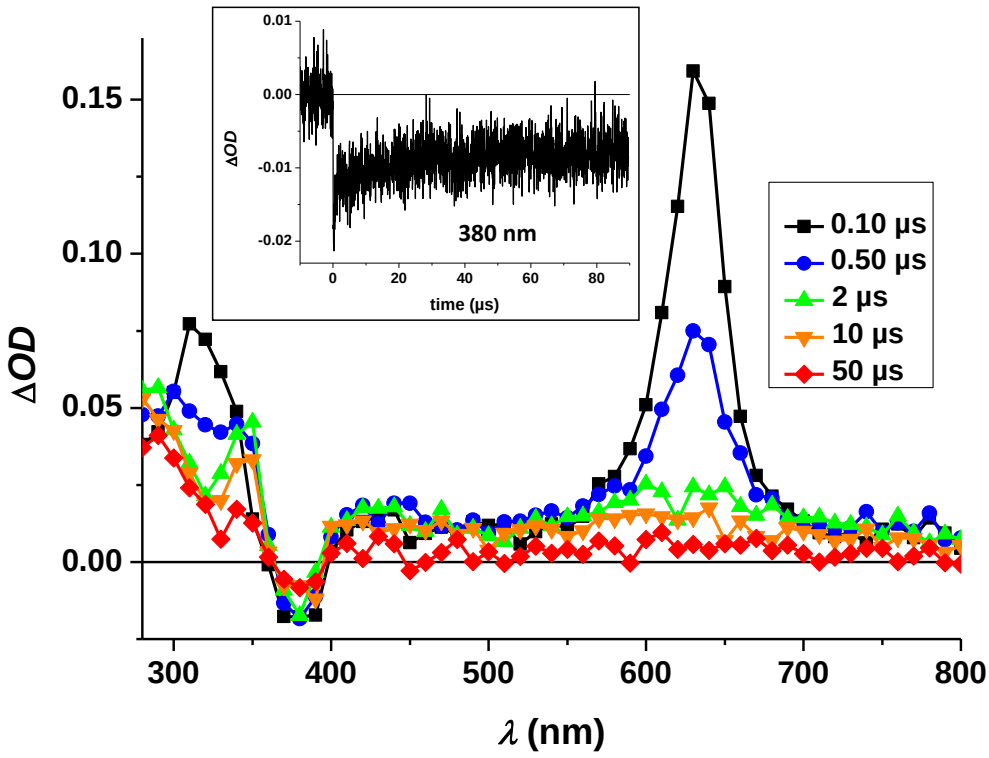


*Figure 2.* Transient absorption spectrum of ITX at different times after laser flash in presence of $1.2 \times 10^{-2}$ M of TS in MeCN ($\lambda_{exc}$ = 355 nm, 4 – 6 mJ/pulse).

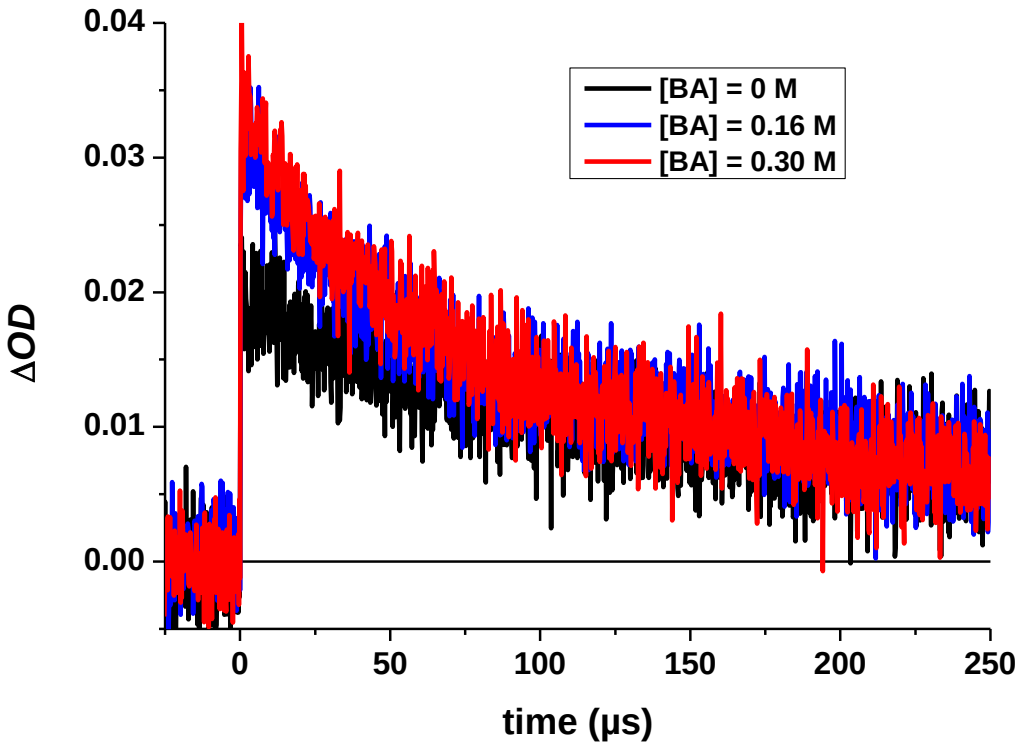


*Figure 3*. Kinetic traces recorded at 300 nm of an argon-saturated solution of TA at different concentrations of butyl acrylate in MeCN ($\lambda_{exc}$ = 355 nm, 18 – 20 mJ/pulse).

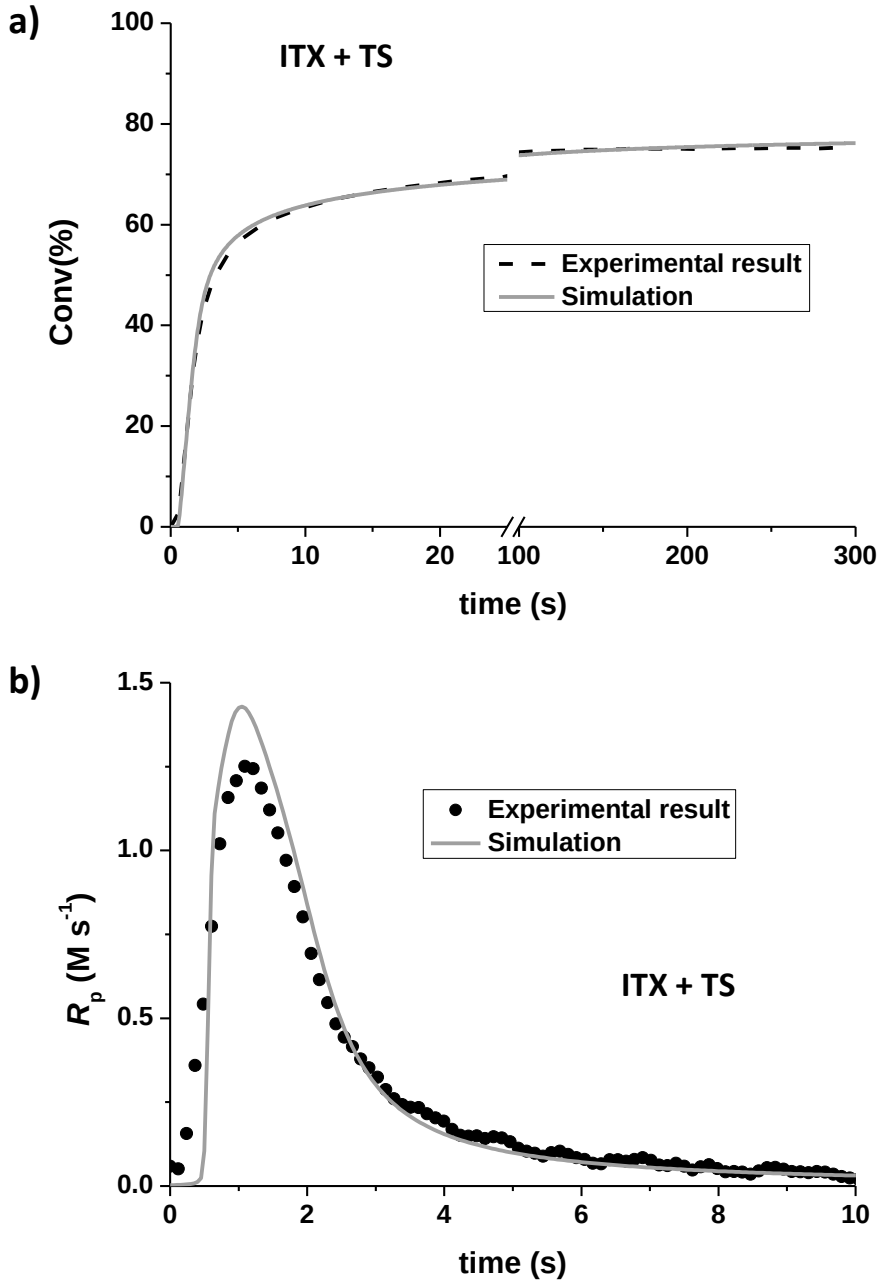


*Figure 4*. Comparison between experimental (black dashed) and simulated (grey plain) acrylate double bond for a) conversion and b) rate of polymerization, assuming $k_q = k_d$ upon LED exposure at 395 nm (irradiance = 10 mW cm$^{-2}$) – ITX / TS (0.1 wt% / 1.5 × 10$^{-2}$ M) in SR349 + 10 wt% DMSO.

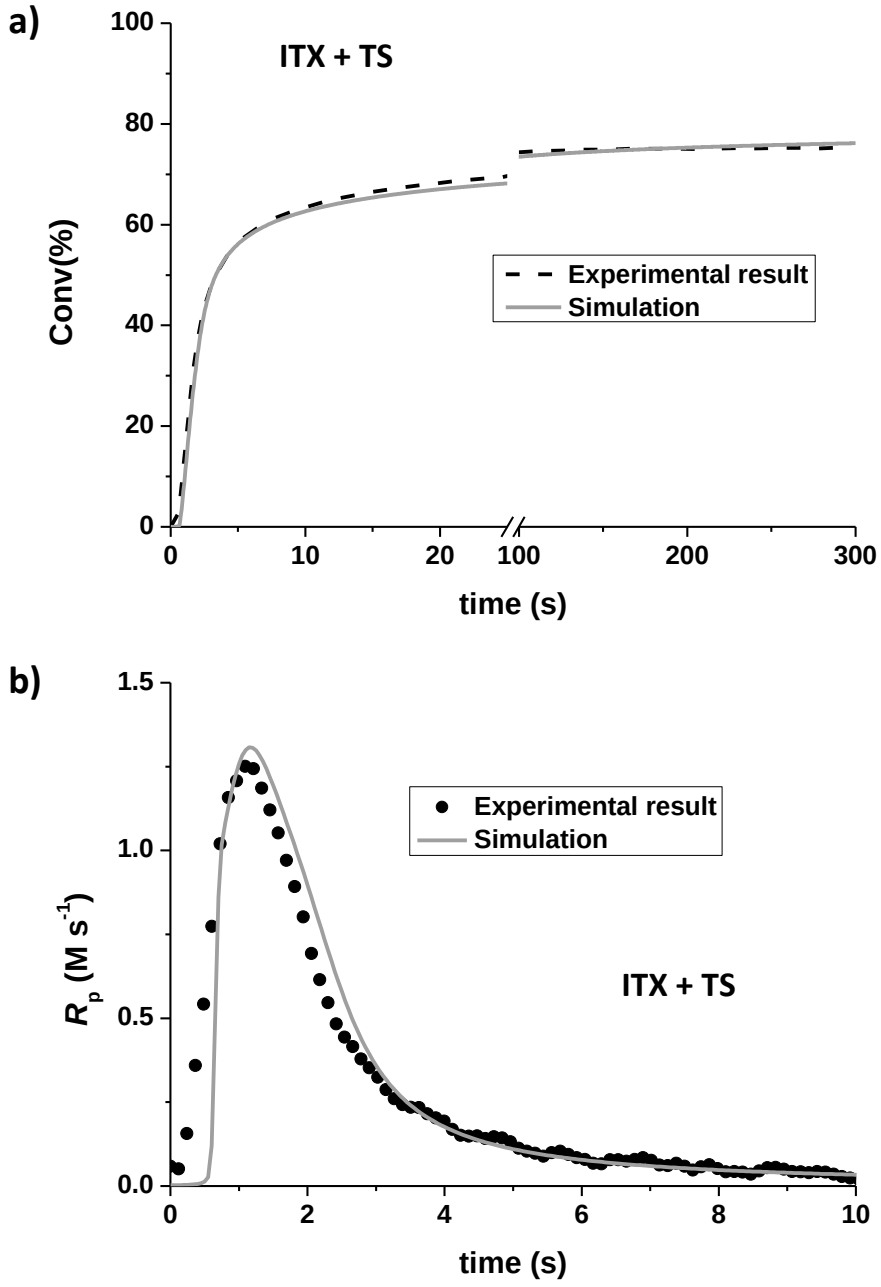


*Figure 5*. Comparison between experimental (black dashed) and simulated (grey plain) acrylate double bond for a) conversion and b) rate of polymerization, taking into account mechanism of Scheme 3 upon LED exposure at 395 nm (irradiance = 10 mW cm$^{-2}$) – ITX / TS (0.1 wt% / 1.5 × 10$^{-2}$ M) in SR349 + 10 wt% DMSO.

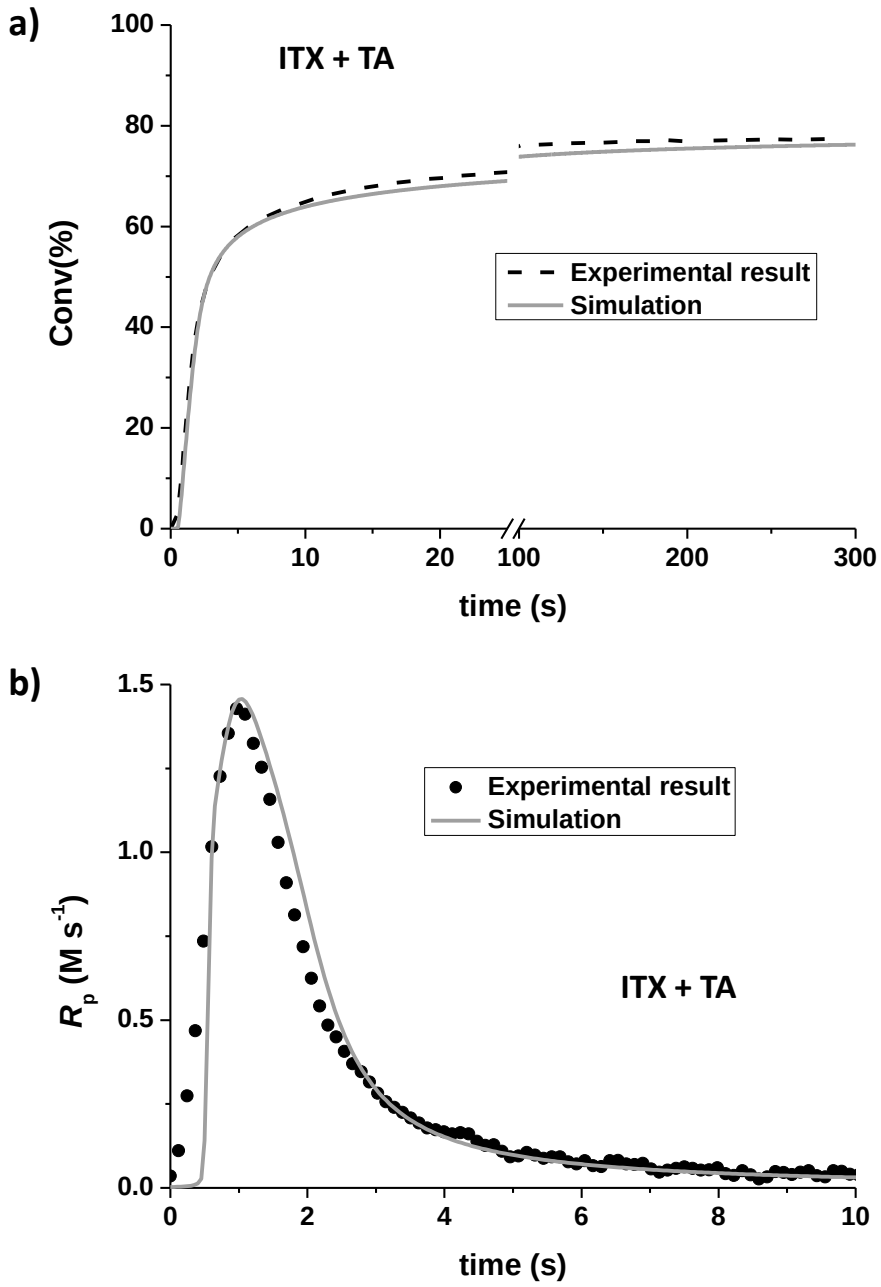


*Figure 6*. Comparison between experimental (black dashed) and simulated (grey plain) acrylate double bond for a) conversion and b) rate of polymerization, taking into account mechanism of Scheme 3 upon LED exposure at 395 nm (irradiance = 10 mW cm$^{-2}$) – ITX / TA (0.1 wt% / 1.5 × 10$^{-2}$ M) in SR349 + 10 wt% DMSO.

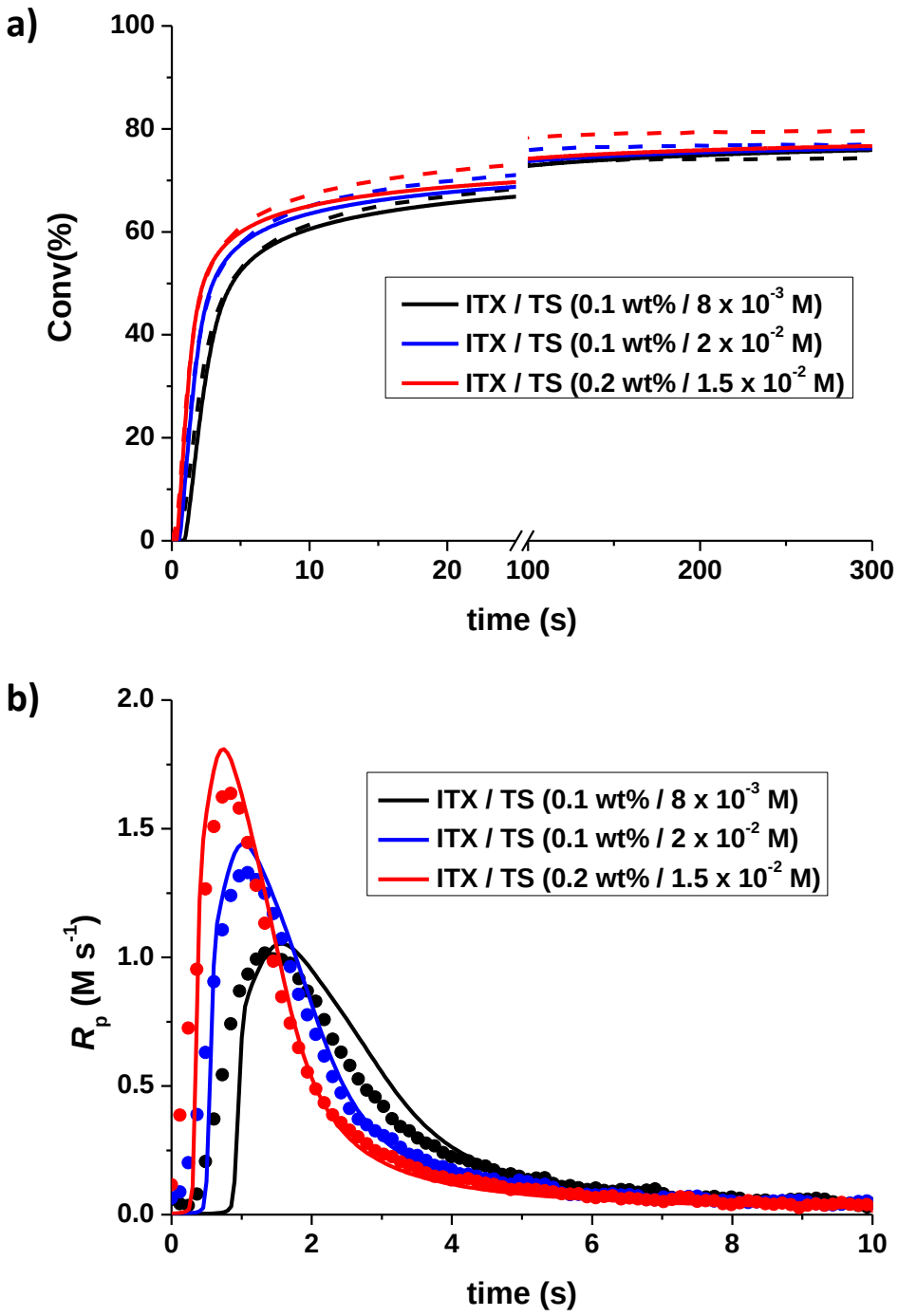


*Figure 7*. Comparison of experimental (dashed) and simulated (plain) acrylate double bond for a) conversion and b) rate of polymerization upon LED exposure at 395 nm (irradiance = 10 mW $cm^{-2}$), with various initial amounts of ITX and TS.

ToC abstract:

**The photochemical mechanism of a new Type-II photoiniating system based on isopropylthioxanthone (ITX) and a triazine derivative is investigated by time-resolved spectroscopy.** More insights in that mechanism are obtained through the kinetic modeling of the free radical photopolymerization process initiated by this two-component system. It reveals the importance of back electron transfer in such a mechanism.

ToC figure: